WIRELESS COMMUNICATIONS AND MOBILE COMPUTING
Wirel. Commun. Mob. Comput. 2013; **13**:1435–1449
Published online 4 September 2011 in Wiley Online Library (wileyonlinelibrary.com). DOI: 10.1002/wcm.1191

RESEARCH ARTICLE

Optimal and suboptimal receivers for code-multiplexed transmitted-reference ultra-wideband systems†

Mehmet Emin Tutay and Sinan Gezici*

Department of Electrical and Electronics Engineering, Bilkent University, Bilkent, Ankara TR-06800, Turkey

ABSTRACT

In this study, optimal and suboptimal receivers are investigated for code-multiplexed transmitted-reference (CM-TR) ultra-wideband systems. First, a single-user scenario is considered, and a CM-TR system is modeled as a generalized noncoherent pulse-position modulated system. Based on that model, the optimal receiver that minimizes the bit error probability is derived. Then, it is shown that the conventional CM-TR receiver converges to the optimal receiver under certain conditions and achieves close-to-optimal performance in practical cases. Next, multi-user systems are considered, and the conventional receiver, blinking receiver, and chip discriminator are investigated. Also, the linear minimum mean-squared error (MMSE) receiver is derived for the downlink of a multi-user CM-TR system. In addition, the maximum likelihood receiver is obtained as a performance benchmark. The practicality and the computational complexity of the receivers are discussed, and their performance is evaluated via simulations. The linear MMSE receiver is observed to provide the best trade-off between performance and complexity/practicality. Copyright © 2011 John Wiley & Sons, Ltd.

KEYWORDS

ultra-wideband (UWB); code-multiplexed transmitted-reference (CM-TR); maximum likelihood (ML); chip discriminator; minimum mean-squared error (MMSE)

***Correspondence**

Sinan Gezici, Department of Electrical and Electronics Engineering, Bilkent University, Bilkent, Ankara TR-06800, Turkey.
E-mail: gezici@ee.bilkent.edu.tr

1. INTRODUCTION

In addition to high-speed data transmission [1] and accurate position estimation [2], pulse-based ultra-wideband (UWB) signals can also facilitate low-to-medium rate data communications with low-power and low-cost transceivers. In order to realize such low-power/cost implementations, one can consider transmitted-reference (TR) UWB systems, in which a pair of signals that are time-delayed versions of each other are transmitted for each information symbol [3,4]. A TR UWB receiver uses one of those signals as a *reference* ('template') signal for the other one (called the *data* signal) to estimate the transmitted information. The main advantages of TR UWB receivers are that there is no need to estimate individual channel coefficients and template signals, which is quite challenging for UWB systems, and that the receiver can be operated based on symbol-rate or frame-rate samples. However, the main disadvantage of TR UWB receivers is related to the need for an analog delay line to perform data demodulation [3,5].

In order to realize the advantages of TR UWB systems without the need for an analog delay line, slightly frequency-shifted reference (FSR) UWB systems are proposed, which employ data and reference pulses that are shifted in the frequency-domain instead of the time-domain [5]. One limitation of FSR UWB systems is that the orthogonality between the data and reference signals cannot be maintained at the receiver for high-data rate systems [6]. Therefore, there is an inherent data rate limitation in these systems.

Instead of employing time-delayed or frequency-shifted versions of two signals as in TR UWB and FSR UWB systems, respectively, one can consider sending those two signals at the same time and frequency, but orthogonalizing them by means of certain codes [6–11]. Specifically,

†Part of this work was presented at IEEE International Conference on Ultra-Wideband (ICUWB), vol. 3, pp. 117–120, Sep. 10–12, 2008.

reference and data signals can be made orthogonal by coding the polarity of pulses in each signal. Such systems, called code-multiplexed transmitted-reference (CM-TR) UWB systems [7], provide advantages over both the TR UWB and FSR UWB systems. Similar to FSR UWB, CM-TR UWB systems do not need analog delay lines, and they also have better bit error probability (BEP) performance than FSR UWB and TR UWB systems [7]. In addition, they do not have the data rate limitation that FSR UWB systems experience [6].

Single-user CM-TR UWB systems are investigated in [6] and [7], and the advantages of a CM-TR UWB receiver are discussed in terms of implementation complexity and BEP performance. In [8], the timing acquisition is studied for CM-TR UWB systems, and it is shown that the synchronization can be performed quickly in a simple manner. CM-TR UWB systems are investigated for multi-user environments in [12], their performance is compared with that of the TR UWB system that employs orthogonal sequences for inter-pulse interference cancelation [13,14] and that of the FSR UWB system. It is shown that the CM-TR UWB achieves the best performance and the lowest implementation complexity.

Although CM-TR UWB systems have been investigated in single-user and multi-user environments [6,7,12], the optimality of the employed receiver structure has not been investigated, and alternative optimal and suboptimal receivers for multi-user systems have not been considered in the literature. In this paper, optimal and suboptimal receivers are studied for CM-TR UWB systems. For single-user systems, the optimal receiver is derived, and it is shown that the conventional CM-TR UWB receiver in [7] converges to the optimal receiver under certain conditions. In other words, the conventional receiver is shown to provide a low-cost solution that is close-to-optimal for practical system parameters. In addition, the interpretation of the conventional CM-TR receiver as a generalized noncoherent pulse-position demodulator is provided. For multi-user systems, various receivers with different levels of computational complexity are studied for the downlink of a CM-TR system. In order to improve the performance of the conventional CM-TR receiver in certain multi-user environments, the blinking receiver (BR) and the chip discriminator [15] are investigated, which discard energy samples with (significant) interference in the calculation of the decision variable. In addition, the linear minimum mean-squared error (MMSE) receiver is proposed in order to optimally combine the energy samples obtained from different frames. The linear MMSE receiver is shown to provide significant performance improvements over the conventional receiver, the BR, and the chip discriminator. Furthermore, the maximum likelihood (ML) receiver is obtained in order to provide a performance benchmark for the other receivers. The practicality and the computational complexity of all the receivers are discussed, and the linear MMSE receiver is shown to be a practical choice with good performance.

The remainder of the paper is organized as follows. Section 2 introduces a generic signal model for TR, FSR, and CM-TR UWB systems and provides a received signal model for a multi-user CM-TR UWB system. In Section 3, the single-user case is investigated, the conventional and the optimal receivers are studied, and the asymptotic optimality property of the conventional receiver is discussed. The multi-user systems are studied in Section 4, and various receiver structures are investigated. Finally, concluding remarks are made in Section 5.

2. SIGNAL MODEL

First, a generic signal structure is defined, which covers TR, FSR, and CM-TR UWB signals as special cases. The transmitted signal corresponding to symbol 0 of the kth user is given by

$$s^{(k)}(t) = \sqrt{\frac{E_k}{2N_f}} \sum_{j=0}^{N_f-1} \left[a_j^{(k)} \omega \left(t - j T_f - c_j^{(k)} T_c \right) + b^{(k)} a_j^{(k)} \omega \left(t - j T_f - c_j^{(k)} T_c - T_d \right) x(t) \right], \quad (1)$$

for $t \in [0, T_s]$, where T_s, T_f, and T_c are, respectively, the symbol, frame, and chip intervals, N_f is the number of frames per symbol, E_k is the symbol energy for user k, $\omega(t)$ is the UWB pulse with unit energy, and $b^{(k)} \in \{-1, +1\}$ is the binary information symbol for symbol 0 of user k.[‡] In order to increase robustness against multiple access interference [16] and avoid spectral lines [17], polarity randomization codes $a_j^{(k)} \in \{-1, +1\}$ are employed. In addition, a time-hopping (TH) code $c_j^{(k)} \in \{0, 1, \ldots, N_c - 1\}$ is assigned to each user in order to reduce the probability of simultaneous collisions between the pulses of multiple users in different frames [18].

Depending on the selection of T_d and $x(t)$, the signal model in (1) reduces to TR, FSR, and CM-TR systems as follows:

- For TR systems, T_d represents the time-delay between the reference and data pulses in each frame, and $x(t) = 1 \ \forall t$.
- For FSR systems, $T_d = 0$ and $x(t) = \sqrt{2}\cos(2\pi f_0 t)$, which provides a slight frequency shift to the data pulses [5].
- For CM-TR systems, $T_d = 0$ and $x(t)$ is given by

$$x(t) = \sum_{j=0}^{N_f-1} \tilde{d}_j^{(k)} \, p\left(t - j T_f\right) , \quad (2)$$

where $p(t) = 1$ for $t \in [0, T_f]$ and $p(t) = 0$ otherwise, and $\tilde{d}_j^{(k)} \in \{-1, +1\}$ is the jth element of the code for user k that provides *orthogonalization* of the data and reference pulses at the receiver [7].

[‡]For convenience, the symbol index 0 is not shown in $s^{(k)}(t)$.

Transmitted-reference systems provide orthogonalization of data and reference signals by separating them in the time-domain, whereas FSR systems facilitate separation via a shift in the frequency-domain. On the other hand, the approaches in [6] and [7] propose a separation in the code domain, which has significant advantages over the previous techniques in terms of performance and/or implementation complexity [7,12].

From (2), (1) can be expressed as

$$s^{(k)}(t) = \sqrt{\frac{E_k}{2N_\mathrm{f}}} \sum_{j=0}^{N_\mathrm{f}-1} a_j^{(k)} \left(1 + b^{(k)} \tilde{d}_j^{(k)}\right) \times \omega\left(t - j\,T_\mathrm{f} - c_j^{(k)} T_\mathrm{c}\right) . \quad (3)$$

Note that $a_j^{(k)} \left(1 + b^{(k)} \tilde{d}_j^{(k)}\right)$ takes a value from the set $\{-2, 0, +2\}$.

Assume that the signal in (3) passes through a multipath channel with the channel impulse response $h_c(t) = \sum_{l=1}^{L} \rho_l\, \delta(t - \tau_l)$, where ρ_l and τ_l represent, respectively, the channel coefficient and delay of the lth path. Then, the received signal in a K-user system can be expressed from (3) as

$$r(t) = \sum_{k=1}^{K} r_k(t) + n(t) , \quad (4)$$

with

$$r_k(t) = \sqrt{\frac{E_k}{2N_\mathrm{f}}} \sum_{j=0}^{N_\mathrm{f}-1} a_j^{(k)} \left(1 + b^{(k)} \tilde{d}_j^{(k)}\right) \times \tilde{\omega}\left(t - j\,T_\mathrm{f} - c_j^{(k)} T_\mathrm{c}\right) , \quad (5)$$

where $\tilde{\omega}(t) = \sum_{l=1}^{L} \rho_l\, \omega(t - \tau_l)$ and $n(t)$ is the zero mean Gaussian noise with a a flat spectral density of σ^2 over the system bandwidth (B). It is assumed that the frame interval is sufficiently long and the TH codes are selected in such a way that there occurs no inter-frame interference (IFI) [6]. Note that because of the no IFI assumption, signal demodulation can be performed symbol-by-symbol without loss of optimality. Hence, only one symbol is considered in (5).

For the theoretical analysis in the following sections, perfect synchronization is assumed, which is a common assumption in the literature for the analysis of CM-TR systems [6,7,12]. The main reason for this simplifying assumption is that because CM-TR receivers employ noncoherent detection, practical range of synchronization errors do not commonly have significant effects on the BEP. In other words, precise synchronization is not crucial for CM-TR systems, as stated in [19]. Therefore, for theoretical studies, it is convenient to assume that the synchronization has been achieved by a conventional algorithm (such as that in [7] or [8]), and the synchronization errors are negligible.

3. SINGLE-USER CASE

In this section, single-user systems are studied, and the conventional receiver [6,7] for such systems is investigated. Also, an optimal receiver that minimizes the average probability of error is derived, and the asymptotic optimality properties of the conventional receiver are studied.

3.1. Conventional receiver

For a single-user system, the received signal in (4) and (5) becomes

$$r(t) = \sqrt{\frac{E_1}{2N_\mathrm{f}}} \sum_{j=0}^{N_\mathrm{f}-1} a_j\,(1 + b\,\tilde{d}_j)\,\tilde{\omega}(t - j\,T_\mathrm{f} - c_j\,T_\mathrm{c}) + n(t), \quad (6)$$

where the user superscript is dropped for convenience. In order to estimate the information symbol b from the received signal in (6), the orthogonality between the reference and data pulses is utilized [6,7]. Namely, the information symbol is estimated as

$$\hat{b} = \mathrm{sgn}\left\{\int_0^{T_\mathrm{s}} r^2(t)\, x(t)\, \mathrm{d}t\right\} , \quad (7)$$

where $\mathrm{sgn}\{\cdot\}$ represents the sign operator. The detector in (7) can be implemented as shown in the first receiver structure in Figure 1. From (2), (7) can also be expressed as

$$\hat{b} = \mathrm{sgn}\left\{\sum_{j=0}^{N_\mathrm{f}-1} \tilde{d}_j \int_{j\,T_\mathrm{f}}^{(j+1)T_\mathrm{f}} r^2(t)\, \mathrm{d}t\right\} , \quad (8)$$

which suggests another detector implementation based on frame-rate samples [7], as illustrated in the second structure in Figure 1.

Although both receivers in Figure 1 can be considered in the framework of CM-TR signals [6,7], it is also possible to consider the current system as a 'generalized' pulse-position modulation (PPM) system. To that end, define $\mathcal{S}$ and $\bar{\mathcal{S}}$ as the sets of frame indices for which $\tilde{d}_j = 1$ and $\tilde{d}_j = -1$, respectively; that is,

$$\mathcal{S} = \left\{j \in \mathcal{F} \,|\, \tilde{d}_j = 1\right\} , \quad \bar{\mathcal{S}} = \left\{j \in \mathcal{F} \,|\, \tilde{d}_j = -1\right\} , \quad (9)$$

where $\mathcal{F} = \{0, 1, \ldots, N_\mathrm{f} - 1\}$ is the set of frame indices. Note that $\mathcal{S} \cup \bar{\mathcal{S}} = \mathcal{F}$. In addition, both sets include $N_\mathrm{f}/2$ indices for orthogonalization purposes [7]; that is, $|\mathcal{S}| = |\bar{\mathcal{S}}| = N_\mathrm{f}/2$.

Note that for $b = 1$, the pulses are transmitted in the frames indexed by $\mathcal{S}$, and no pulses are transmitted in the frames indexed by $\bar{\mathcal{S}}$ (see (6)). Similarly, for $b = -1$, the pulses are transmitted in the frames indexed by $\bar{\mathcal{S}}$ and no pulses are transmitted in the frames indexed by $\mathcal{S}$.

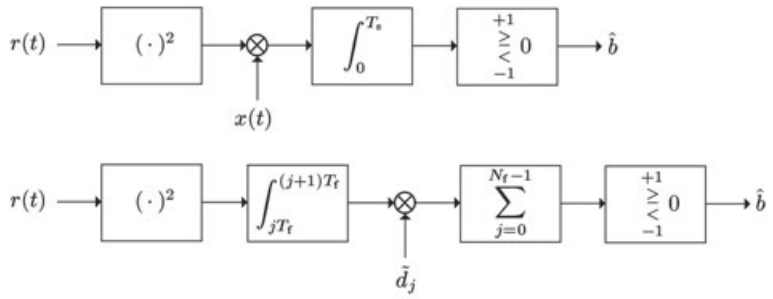

Figure 1. Receivers for single-user code-multiplexed transmitted-reference ultra-wideband systems. The first receiver employs symbol-rate sampling, whereas the second one uses frame-rate sampling.

Also, it is observed from (8) that comparing the sum of N_f outputs against zero is equivalent to comparing the sum of the positive outputs against the absolute value of the sum of the negative outputs. Therefore, (8) can be expressed, using (9), as

$$\mathcal{H}_0 : y_j = \begin{cases} \int_0^{T_f} n_j^2(t)\,\mathrm{d}t\,, & j \in \mathcal{S} \\ \int_0^{T_f} \left[\omega_j(t) + n_j(t)\right]^2 \mathrm{d}t\,, & j \in \bar{\mathcal{S}} \end{cases}, \quad \mathcal{H}_1 : y_j = \begin{cases} \int_0^{T_f} \left[\omega_j(t) + n_j(t)\right]^2 \mathrm{d}t\,, & j \in \mathcal{S} \\ \int_0^{T_f} n_j^2(t)\,\mathrm{d}t\,, & j \in \bar{\mathcal{S}} \end{cases} \tag{11}$$

$$\sum_{j\in\mathcal{S}} \int_{jT_f}^{(j+1)T_f} r^2(t)\,\mathrm{d}t \underset{\hat{b}=-1}{\overset{\hat{b}=+1}{\gtrless}} \sum_{j\in\bar{\mathcal{S}}} \int_{jT_f}^{(j+1)T_f} r^2(t)\,\mathrm{d}t\,, \tag{10}$$

which is similar to a noncoherent binary PPM detector. However, unlike conventional PPM systems [20], the signals employed for the binary symbols are not always time-shifted versions of each other in an CM-TR system, since each signal consists of a number of pulses in different frames of the CM-TR symbol. Therefore, combining the energies of pulses in different frames is an important issue in CM-TR systems, as discussed in Section 4.

3.2. Maximum likelihood receiver and asymptotic optimality of conventional receiver

In order to investigate the optimality of the conventional CM-TR UWB receiver studied in the previous section, we first derive the ML receiver, which minimizes the average probability of error for equiprobable information symbols [21].

Let $y_j = \int_{jT_f}^{(j+1)T_f} r^2(t)\,\mathrm{d}t$, $j = 0, 1, \ldots, N_f - 1$, represent the set of energy samples obtained from different frames. Then, from (6) and (9), the optimal receiver design problem can be modeled as the following binary hypothesis testing problem

$$\mathcal{H}_0 : y_j \sim \begin{cases} \chi^2_M(0)\,, & j \in \mathcal{S} \\ \chi^2_M(\theta)\,, & j \in \bar{\mathcal{S}} \end{cases}, \quad \mathcal{H}_1 : y_j \sim \begin{cases} \chi^2_M(\theta)\,, & j \in \mathcal{S} \\ \chi^2_M(0)\,, & j \in \bar{\mathcal{S}} \end{cases} \tag{12}$$

where $\mathcal{H}_0$ and $\mathcal{H}_1$ represent the $b = -1$ and $b = 1$ hypotheses, respectively, $\omega_j(t) \triangleq \sqrt{\frac{2E_1}{N_f}}\, a_j\, \tilde{\omega}(t)$, and $n_j(t) \triangleq n(t + jT_f)$.

Because $n(t)$ is zero mean Gaussian noise with a flat spectral density of σ^2 over the system bandwidth, the energy samples can be shown to be distributed as central and noncentral chi-square random variables [22]. Therefore, (11) can be expressed as

where M is the approximate dimensionality of the signal space, which is obtained from the time-bandwidth product [22], θ is the signal energy (in the absence of noise), which can be obtained as $\theta = 2E_1E_\omega/N_f$, with $E_\omega = \int_{-\infty}^{\infty} \tilde{\omega}^2(t)\,\mathrm{d}t$, and $\chi^2_M(\theta)$ denotes a noncentral chi-square distribution with M degrees of freedom and a noncentrality parameter of θ. Clearly, $\chi^2_M(\theta)$ reduces to a central chi-square distribution with M degrees of freedom for $\theta = 0$. For the model in (12), it is assumed that the noise components are independent for energy samples from different frames.[§]

From (12), the optimal receiver can be obtained as in the following proposition.

[§]This is approximately true in practice because the frame interval is commonly much larger than the inverse of the bandwidth.

Proposition 1. *For equiprobable information symbols, the probability of error is minimized by the following ML decision rule:*

$$\prod_{j\in\mathcal{S}} y_j^{\frac{1}{2}-\frac{M}{4}} \mathrm{I}_{\frac{M}{2}-1}\left(\frac{\sqrt{\theta y_j}}{\sigma^2}\right) \underset{\hat{b}=-1}{\overset{\hat{b}=+1}{\gtrless}} \prod_{j\in\bar{\mathcal{S}}} y_j^{\frac{1}{2}-\frac{M}{4}} \times \mathrm{I}_{\frac{M}{2}-1}\left(\frac{\sqrt{\theta y_j}}{\sigma^2}\right), \tag{13}$$

where $\mathrm{I}_\nu(x)$ *for* $x \geq 0$ *is the* ν*-th order modified Bessel function of the first kind.*

Proof. Please see Appendix A.

Comparison of (10) and (13) reveals that the conventional receiver in (10) has lower computational complexity than the optimal one because it directly adds up the signal energies in different frames. In addition, the optimal receiver requires the knowledge of θ, which is not readily available in practice. Therefore, the BEP performance of the optimal receiver can be considered to provide a lower bound on that of the conventional receiver.

Before comparing the performance of the conventional receiver with that of the optimal ML receiver, the asymptotic optimality of the conventional approach will be established in the following. To that end, the following result is obtained first.

Lemma 1. *If* M *is an even number, the optimal receiver in (13) can be expressed as*

$$\sum_{j\in\mathcal{S}} \log\left(1+\sum_{l=1}^{\infty} k_l \theta^l y_j^l\right) \underset{-1}{\overset{+1}{\gtrless}} \sum_{j\in\bar{\mathcal{S}}} \log\left(1+\sum_{l=1}^{\infty} k_l \theta^l y_j^l\right) \tag{14}$$

where

$$k_l \triangleq \left[\left(2\sigma^2\right)^{2l} l!\left(\frac{M}{2}\right)\cdots\left(\frac{M}{2}+l-1\right)\right]^{-1} \quad \text{for } l=1,2,\ldots \tag{15}$$

Proof. Please see Appendix B.

The main implication of Lemma 1 related to the asymptotic optimality of the conventional receiver follows from the observation that for large M values, the logarithm terms in (14) converge to $\theta y_j/(2M\sigma^4)$; hence, the test reduces to (10). In other words, if the chi-square random variables representing the signal energies in different frames have large degrees of freedom, then the conventional receiver performs very closely to the optimal one. Note that the degrees of freedom parameter is determined by the product of the bandwidth and the observation interval [22]. Therefore, as the integration interval over which the energy is calculated (in this case, the frame interval, T_f) increases, M also increases. Note that in practice, the integration can be performed over intervals that are smaller than the frame interval in order to collect less noise and increase the signal-to-noise ratio (SNR) [23]. Therefore, the performance of the conventional receiver should be investigated for various M values in order to determine how close it gets to the optimal receiver in various scenarios, which is studied next.

3.3. Numerical results

In this section, the performance of the conventional receiver in (10) is compared with that of the optimal ML receiver in (13) for various system parameters. For the first set of simulations, $\theta = 10$, the number of frames, N_f, is equal to 10, σ^2 is set to unity, and the TH codes are $c_j = 0$, $\forall j$. In order to investigate the performance of the receivers for various degrees of freedom, BEPs are obtained for various M values. For each M, the frame interval and/or the bandwidth are adjusted to provide the desired M and no IFI exists in any of the scenarios. Figure 2 illustrates the BEPs of the two receivers. Although the optimal ML receiver performs better than the conventional receiver for small M, the performance difference is not significant, and the receivers have almost the same performance for $M \geq 8$. The same simulations are performed also for $N_\mathrm{f} = 4$ and $\theta = 25$, and $N_\mathrm{f} = 10$ and $\theta = 20$. The results are shown on the same plot in Figure 2. As in the previous scenario, the conventional receiver performs very closely to the optimal ML receiver. In addition, lower BEPs are observed compared with the previous scenario.

In Figure 2, BEPs increase with M, which is because of the fact that the noise power gets higher as M increases. In other words, because M increases as the system bandwidth or the integration interval increases, more noise is collected by the receiver for a higher value of M. Hence, for a given signal energy, the SNR decreases with M. This relation can also be observed from the BEP expressions in [7,24].

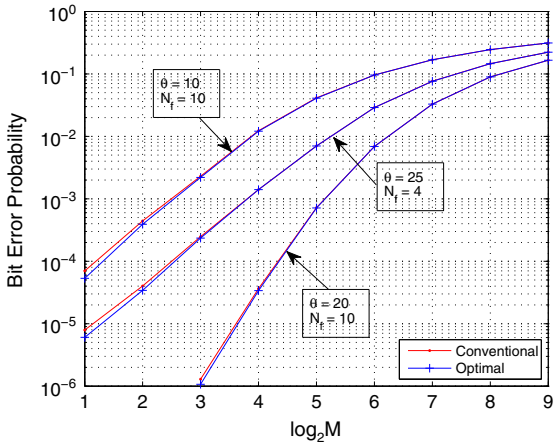

Figure 2. Bit error probability versus M for the conventional and the optimal receivers in single-user code-multiplexed transmitted-reference ultra-wideband systems.

It follows from both the simulations and the theoretical analysis that the conventional receiver converges to the optimal ML receiver for sufficiently large M values in single-user CM-TR UWB systems. Because M is determined by the multiplication of the signal bandwidth and the integration interval for the frames, larger integration intervals guarantee that the conventional receiver performs very closely to the optimal one. In practice, UWB channels commonly have large delay spreads; hence, the integration interval cannot be made very small compared with the pulse width. Therefore, in practical cases, M is not expected to be very small, and the conventional receiver has almost the optimal performance. Also, note that the conventional receiver has lower computational complexity than the optimal one and it makes almost no assumptions about the signal parameters. Hence, the conventional receiver seems to be a natural choice for demodulating CM-TR UWB signals for the considered system settings in a single-user scenario. However, the situation is quite different for multi-user systems, as investigated next.

4. MULTI-USER CASE

In this section, optimal and suboptimal receivers are studied for the downlink of a multi-user CM-TR UWB system. First, low-complexity receivers are investigated. Then, a linear MMSE receiver is derived. In order to provide a performance benchmark, the ML receiver is also obtained. Performance of the receivers is investigated via simulations, and the practicality of each receiver is discussed.

In order to provide a generic framework, define y_j as the energy sample obtained by the user of interest (say, user 1) in the jth frame; that is,

$$y_j = \int_{\Gamma_j} r^2(t)\,\mathrm{d}t \tag{16}$$

for $j = 0, 1, \ldots, N_\mathrm{f} - 1$, where Γ_j denotes the integration interval for frame j. Although the selection of the integration interval commonly depends on the TH code of user 1, the dependence of Γ_j (and y_j) on the user index is not explicitly shown for notational convenience. In the following, we investigate various receivers, which employ $y_0, y_1, \ldots, y_{N_\mathrm{f}-1}$ as the inputs and provide a bit estimate as the output.

4.1. Conventional receiver

The conventional receiver in (10) for a single-user system can also be employed by each user in a multi-user system based on the energy samples in (16) [12]. Considering user 1 as the user of interest, the conventional receiver determines the information bit as follows:

$$\sum_{j\in\mathcal{S}_1} y_j \underset{\hat{b}^{(1)}=-1}{\overset{\hat{b}^{(1)}=+1}{\gtrless}} \sum_{j\in\bar{\mathcal{S}}_1} y_j\,, \tag{17}$$

where $\mathcal{S}_1 = \{j \in \mathcal{F} \mid \tilde{d}_j^{(1)} = 1\}$ and $\bar{\mathcal{S}}_1 = \{j \in \mathcal{F} \mid \tilde{d}_j^{(1)} = -1\}$, as in (9). Although the conventional receiver is approximately optimal for single-user systems, it will be shown in this section that it can have very poor performance in multi-user scenarios and perform significantly worse than the optimal detector.

4.2. Blinking receiver and chip discriminator

The main problem with the conventional receiver in a multi-user system is that comparing the sum of the energy samples as in (17) can become quite unreliable when the pulses of the user of interest collide with those of the other users. For this reason, the BR and the chip discriminator discard some of the colliding pulses of the user of interest and estimate the transmitted information bit based on uncorrupted or slightly corrupted pulses [15,25,26]. If the number of pulses with slight or no collision is sufficiently high per information symbol, these two receivers can perform significantly better than the conventional receiver.

The BR and the chip discriminator estimate the transmitted bit of the user of interest (user 1) based on the following decision rule[¶]

$$\frac{\sum\limits_{j\in\mathcal{S}_1} \beta_j\, y_j}{\sum\limits_{j\in\mathcal{S}_1} \beta_j} \underset{\hat{b}^{(1)}=-1}{\overset{\hat{b}^{(1)}=+1}{\gtrless}} \frac{\sum\limits_{j\in\bar{\mathcal{S}}_1} \beta_j\, y_j}{\sum\limits_{j\in\bar{\mathcal{S}}_1} \beta_j}\,, \tag{18}$$

where $\mathcal{S}_1$ and $\bar{\mathcal{S}}_1$ are as defined for (17). For the BR, the coefficients β_j are determined as follows:

$$\beta_j = \begin{cases} 1\,, & \text{if } \min\limits_{k\in\{2,\ldots,K\}} \left|c_j^{(1)} - c_j^{(k)}\right| \geq T_\mathrm{ds}/T_\mathrm{c} \\ 0\,, & \text{otherwise} \end{cases}, \tag{19}$$

where $c_j^{(k)}$ is the TH code for the jth frame of user k, T_ds denotes the maximum delay spread [27] of the channel, and T_c is the chip interval. In other words, the weight is set to 1 for frame j if there are no collisions between the pulses of the user of interest and those of the other users. On the other hand, for the chip discriminator, we set β_j as follows:

$$\beta_j = \begin{cases} 1\,, & \text{if } \min\limits_{k\in\{2,\ldots,K\}} \left|c_j^{(1)} - c_j^{(k)}\right| \geq \Delta_1 \\ & \quad \text{or } \frac{\sum_{k=2}^{K} E_k}{E_1} \leq \Delta_2 \\ 0\,, & \text{otherwise} \end{cases}, \tag{20}$$

where Δ_1 is the threshold for the difference between the TH codes of user 1 and the other users, and Δ_2 is the threshold for the ratio between the total energy of the interfering users and the energy of user 1. Threshold

[¶]Note that (18) reduces to the conventional receiver for $\beta_j = 1, \forall j$.

Δ_1 controls the amount of collisions between the pulses, whereas Δ_2 determines the significance of the interference level. In this way, the chip discriminator employs the energy sample from a frame in the decision process if the pulses of user 1 are sufficiently separated from those of the other users in that frame, or if the total energy of the interfering users is significantly lower than that of user 1. Therefore, unlike the BR, the chip discriminator takes pulses with low levels of interference into account, as well.

In practical UWB systems, a large number of multipath components are observed at a receiver, and the channel delay spread is significantly larger than the pulse duration [28,29]. For this reason, the BR, which discards all the colliding pulses irrespective of the interference level, can be quite impractical as almost all the pulses of the user of interest can collide with pulses of other users. Therefore, our discussion will focus on the chip discriminator, which in fact covers the BR as a special case when $\Delta_1 = T_{\rm ds}/T_{\rm c}$ and $\Delta_2 = 0$.

Although there are a large number of multipath components in a UWB channel, a significant portion of them are weak components [30,31]. Hence, pulses of user 1 that are interfered by such weak pulses can still be useful in deciding the information bit. Therefore, the chip discriminator should set threshold values Δ_1 and Δ_2 appropriately in order to eliminate only the colliding pulses with strong interference. In other words, the pulses with low levels of interference should be taken into account as well. As an example, consider a two-user system with $E_1 = 1$, $E_2 = 2$, $T_{\rm c} = 1$ ns, and SNR $= 12$ dB. In this case, because the interfering user has twice the energy of the user of interest (i.e., the interference is significant), the second condition in (20) should not be satisfied. Hence, Δ_2 can be any value smaller than 2 in this case. On the other hand, the optimal value of Δ_1 that minimizes the BEP depends on the channel characteristics of the environment. Based on the channel models CM1, CM2, CM3, and CM4 defined in [29], we have performed simulations and obtained that the optimal values of Δ_1 are 14, 20, 10, and 19 for CM1, CM2, CM3, and CM4, respectively. It is noted that these optimal numbers correspond to cases in which pulses can collide to a certain extent.

Compared with the conventional receiver, the chip discriminator can provide significant performance improvements in the presence of strong interference. However, the main disadvantage of the chip discriminator is that it requires the knowledge of the TH codes, the energies of all the users, and the channel delay spread. Also, some knowledge on the channel delay profile is needed in order to determine a suitable value for the threshold parameter Δ_1.

Finally, it should be noted that depending on the number of frames, $N_{\rm f}$, Δ_1, and Δ_2 values, the terms $\sum_{j\in\mathcal{S}}\beta_j$ or $\sum_{j\in\bar{\mathcal{S}}}\beta_j$ in (18) might be zero in some cases. In such scenarios, the conventional receiver ($\beta_j = 1$, $j = 0, 1, \ldots, N_{\rm f}-1$) can be employed. Then, if the number of pulses per information bit, $N_{\rm f}/2$, is low, this receiver can perform closely to the conventional receiver.

4.3. Linear minimum mean-squared error receiver

Because the conventional receiver and the chip discriminator do not have optimality properties for multi-user systems, they can have very poor performance in certain scenarios (see Section 4.5). Therefore, it is desirable to propose a receiver that possesses certain optimality properties and achieves reasonably low error probabilities even in challenging multi-user scenarios. For that purpose, the linear MMSE receiver is obtained in this section. The linear MMSE receiver linearly combines the energy samples in (16) in such a way that the expectation of the square of the difference between that linear combination and the bit of the user of interest, $b^{(1)}$, is minimized. That is,

$$\boldsymbol{\theta}_{\rm MMSE} = \arg\min_{\boldsymbol{\theta}} {\rm E}\left\{\left(\boldsymbol{\theta}^T\mathbf{y} - b^{(1)}\right)^2\right\}, \qquad (21)$$

where $\mathbf{y} = [y_0\ y_1 \cdots y_{N_{\rm f}-1}]^T$ is the vector of energy samples in (16). The MMSE weights are also known to maximize the signal-to-interference-plus-noise ratio of the received signal [32]. Based on the MMSE coefficient $\boldsymbol{\theta}_{\rm MMSE}$, the bit of the user of interest is estimated as the sign of $\boldsymbol{\theta}_{\rm MMSE}^T\mathbf{y}$.

In order to obtain an explicit expression of the linear MMSE receiver, the energy samples in (16) can be expressed based on (4) as

$$\begin{aligned} y_j &= \int_{\Gamma_j} [r_1(t) + r_I(t) + n(t)]^2\, dt \\ &= \int_{\Gamma_j} [r_1(t)]^2\, dt + 2\int_{\Gamma_j} r_1(t)\,[r_I(t) + n(t)]\, dt \\ &\quad + \int_{\Gamma_j} [r_I(t) + n(t)]^2\, dt\,, \end{aligned} \qquad (22)$$

where $r_I(t)$ is the sum of all the interfering signals; that is,

$$r_I(t) = \sum_{k=2}^{K} r_k(t)\,. \qquad (23)$$

In the absence of IFI, the received signal from user k during the jth frame can be expressed from (5) as

$$\begin{aligned} r_k^j(t) = \sqrt{\frac{E_k}{2N_{\rm f}}}\, a_j^{(k)} \left(1 + b^{(k)}\,\tilde{d}_j^{(k)}\right) \\ \times \tilde{\omega}\left(t - jT_{\rm f} - c_j^{(k)}T_{\rm c}\right) \\ \text{for } t \in [jT_{\rm f}, (j+1)T_{\rm f})\,. \end{aligned} \qquad (24)$$

Then, (22) can be written as

$$y_j = \frac{E_1}{2N_f}\left(2 + 2b^{(1)}\tilde{d}_j^{(1)}\right) \times \int_{\Gamma_j} \tilde{\omega}^2\left(t - jT_f - c_j^{(1)}T_c\right)dt + 2\sqrt{\frac{E_1}{2N_f}}\,a_j^{(1)}\left(1 + b^{(1)}\tilde{d}_j^{(1)}\right) \times \int_{\Gamma_j} \tilde{\omega}\left(t - jT_f - c_j^{(1)}T_c\right) \times [r_I(t) + n(t)]\,dt + \int_{\Gamma_j} [r_I(t) + n(t)]^2\,dt\,. \quad (25)$$

In order to simplify the notation, define

$$\gamma_j^{(1)} \triangleq \int_{\Gamma_j} \tilde{\omega}^2\left(t - jT_f - c_j^{(1)}T_c\right)dt \quad (26)$$

$$\alpha_j \triangleq \frac{E_1\gamma_j^{(1)}}{N_f}\tilde{d}_j^{(1)} + \sqrt{\frac{2E_1}{N_f}}\,a_j^{(1)}\tilde{d}_j^{(1)} \times \int_{\Gamma_j} \tilde{\omega}\left(t - jT_f - c_j^{(1)}T_c\right)[r_I(t) + n(t)]\,dt \quad (27)$$

$$n_j \triangleq \sqrt{\frac{2E_1}{N_f}}\,a_j^{(1)} \int_{\Gamma_j} \tilde{\omega}\left(t - jT_f - c_j^{(1)}T_c\right) \times [r_I(t) + n(t)]\,dt + \int_{\Gamma_j} [r_I(t) + n(t)]^2\,dt\,. \quad (28)$$

Then, (25) can be expressed as

$$y_j = \frac{E_1\gamma_j^{(1)}}{N_f} + b^{(1)}\alpha_j + n_j\,, \quad (29)$$

for $j = 0, 1, \ldots, N_f - 1$. In the vector notation, $\mathbf{y}$ can be stated as

$$\mathbf{y} = \mathbf{k} + b^{(1)}\boldsymbol{\alpha} + \mathbf{n}\,, \quad (30)$$

where $\mathbf{k} = \frac{E_1}{N_f}\left[\gamma_0^{(1)} \cdots \gamma_{N_f-1}^{(1)}\right]^T$, $\boldsymbol{\alpha} = [\alpha_0 \cdots \alpha_{N_f-1}]^T$, and $\mathbf{n} = [n_0 \cdots n_{N_f-1}]^T$.

Based on (30), the MMSE weighting vector in (21) can be calculated as [32]

$$\boldsymbol{\theta}_{\text{MMSE}} = \left(\text{E}\left\{\mathbf{y}\mathbf{y}^T\right\}\right)^{-1}\text{E}\{\boldsymbol{\alpha}\} \quad (31)$$

$$= (\mathbf{k}\mathbf{k}^T + \text{E}\{\mathbf{n}\}\mathbf{k}^T + \mathbf{k}\,\text{E}\{\mathbf{n}^T\} + \text{E}\{\boldsymbol{\alpha}\boldsymbol{\alpha}^T\} + \text{E}\{\mathbf{n}\mathbf{n}^T\})^{-1} \times \text{E}\{\boldsymbol{\alpha}\}. \quad (32)$$

Then, the bit estimate is obtained as

$$\hat{b}^{(1)} = sgn\left\{\boldsymbol{\theta}_{\text{MMSE}}^T\mathbf{y}\right\}\,. \quad (33)$$

From (31) and (33), it is observed that the linear MMSE receiver can be implemented in practice based on an estimate of the correlation matrix of the energy samples, $\text{E}\left\{\mathbf{y}\mathbf{y}^T\right\}$, which can be obtained from a number of previous symbols (or, from training symbols). In addition, the knowledge of $\text{E}\{\boldsymbol{\alpha}\}$ is required to obtain the MMSE coefficients. When the polarity randomization codes $a_j^{(k)}$ are equally likely to be -1 or $+1$, the expectation of the second term in (27) becomes equal to zero. Therefore, $\text{E}\{\boldsymbol{\alpha}\}$ is given by

$$\text{E}\{\boldsymbol{\alpha}\} = \frac{E_1}{N_f}\left[\gamma_0^{(1)}\tilde{d}_0^{(1)} \;\cdots\; \gamma_{N_f-1}^{(1)}\tilde{d}_{N_f-1}^{(1)}\right]\,. \quad (34)$$

In addition, when the same durations are used for the integration intervals for all the frames (which is both practical and reasonable because the same channel impulse response is observed in each frame), the $\gamma_j^{(1)}$ terms become the same for all the frames; that is, $\gamma_j^{(1)} = \gamma^{(1)}$ for $j = 0, 1, \ldots, N_f - 1$. Then,

$$\text{E}\{\boldsymbol{\alpha}\} = \frac{E_1\gamma^{(1)}}{N_f}\left[\tilde{d}_0^{(1)} \;\cdots\; \tilde{d}_{N_f-1}^{(1)}\right]\,. \quad (35)$$

Therefore, in the implementation of the linear MMSE receiver, only the knowledge of the orthogonalization codes of the user of interest, $\tilde{d}_0^{(1)}, \ldots, \tilde{d}_{N_f-1}^{(1)}$, is required, because the constant positive term $E_1\gamma^{(1)}/N_f$ does not affect the result of the sign operation in (33). Hence, the linear MMSE receiver can easily be implemented in practical scenarios.

Although the linear MMSE receiver can be implemented in practice based on an estimate of $\text{E}\{\mathbf{y}\mathbf{y}^T\}$ from previous observations and on the knowledge of the orthogonalization codes of the user of interest, obtaining closed-form expressions for the expectation terms in (32) is also important for the theoretical evaluation of the linear MMSE receiver. In the following lemmas, expressions are provided for $\text{E}\left\{\boldsymbol{\alpha}\boldsymbol{\alpha}^T\right\}$, $\text{E}\{\mathbf{n}\}$, and $\text{E}\left\{\mathbf{n}\mathbf{n}^T\right\}$. The proofs of the lemmas can be found in Appendices C-E of [33].

Lemma 2. *Assume that the polarity randomization codes, $a_j^{(k)}$, $k = 2, \ldots, K$, are independent and identically distributed (i.i.d.) and take values -1 or $+1$ with equal probabilities. Then, $\mathrm{E}\{\alpha_j \alpha_l\}$ can be expressed as*

$$\mathrm{E}\{\alpha_j \alpha_l\} = \begin{cases} \dfrac{E_1^2}{N_\mathrm{f}^2} \gamma_j^{(1)} \gamma_l^{(1)} \tilde{d}_j^{(1)} \tilde{d}_l^{(1)}, & j \neq l \\ \dfrac{E_1^2}{N_\mathrm{f}^2} \left(\gamma_j^{(1)}\right)^2 + \dfrac{2E_1}{N_\mathrm{f}} \left[\displaystyle\sum_{k=2}^{K} \dfrac{E_k}{N_\mathrm{f}} \left(\phi_j^{(1,k)}\right)^2 + \sigma^2 \gamma_j^{(1)} \right], & j = l \end{cases} \tag{36}$$

where

$$\phi_j^{(k,l)} \triangleq \int_{\Gamma_j} \tilde{\omega}\left(t - j T_\mathrm{f} - c_j^{(k)} T_\mathrm{c}\right) \times \tilde{\omega}\left(t - j T_\mathrm{f} - c_j^{(l)} T_\mathrm{c}\right) dt \,. \tag{37}$$

Lemma 3. *Assume that the polarity randomization codes, $a_j^{(k)}$, $k = 2, \ldots, K$, are i.i.d. and take the values -1 or $+1$ with equal probabilities. Then, $\mathrm{E}\{n_j\}$ can be obtained as*

$$\mathrm{E}\{n_j\} = \sum_{k=2}^{K} \frac{E_k}{N_\mathrm{f}} \gamma_j^{(k)} + 2B\sigma^2 |\Gamma_j| \,, \tag{38}$$

where $\gamma_j^{(k)} \triangleq \int_{\Gamma_j} \tilde{\omega}^2\left(t - j T_\mathrm{f} - c_j^{(k)} T_\mathrm{c}\right) dt$ and $|\Gamma_j|$ denotes the length of the integration interval in the jth frame.

Lemma 4. *Assume that the polarity randomization codes, $a_j^{(k)}$, $k = 2, \ldots, K$, are i.i.d. and take the values -1 or $+1$ with equal probabilities. In addition, suppose that the same integration duration is used in all the frames; that is, $|\Gamma_j| = |\Gamma|$ for $j = 0, 1, \ldots, N_\mathrm{f} - 1$. Then, $\mathrm{E}\{n_j n_l\}$ can be approximated by*

$$\mathrm{E}\{n_j n_l\} \approx \begin{cases} 4B^2\sigma^4 |\Gamma|^2 \left(1 + \dfrac{1}{B|\Gamma|}\right) + \displaystyle\sum_{k=2}^{K} \frac{E_k^2}{N_\mathrm{f}^2} \left(1 + \tilde{d}_j^{(k)} \tilde{d}_l^{(k)}\right) \gamma_j^{(k)} \gamma_l^{(k)} \\ + 2B\sigma^2 |\Gamma| \displaystyle\sum_{k=2}^{K} \frac{E_k}{N_\mathrm{f}} \left(\gamma_j^{(k)} + \gamma_l^{(k)}\right) + \sum_{\substack{k_1 \neq k_2 \\ k_1, k_2 > 1}} \frac{E_{k_1} E_{k_2}}{N_\mathrm{f}^2} \gamma_j^{(k_1)} \gamma_l^{(k_2)} \,, & j \neq l \\ 4B^2\sigma^4 |\Gamma|^2 \left(1 + \dfrac{1}{B|\Gamma|}\right) + \displaystyle\sum_{k=2}^{K} \frac{2E_k^2}{N_\mathrm{f}^2} \left(\gamma_j^{(k)}\right)^2 + 4\sigma^2 \sum_{k=2}^{K} \frac{E_k}{N_\mathrm{f}} \left(B|\Gamma| + 1\right) \gamma_j^{(k)} + \\ \displaystyle\sum_{\substack{k_1 \neq k_2 \\ k_1, k_2 > 1}} \frac{E_{k_1} E_{k_2}}{N_\mathrm{f}^2} \left[\gamma_j^{(k_1)} \gamma_j^{(k_2)} + 2\left(\phi_j^{(k_1,k_2)}\right)^2\right] + \frac{2E_1}{N_\mathrm{f}} \left[\sum_{k=2}^{K} \frac{E_k}{N_\mathrm{f}} \left(\phi_j^{(1,k)}\right)^2 + \sigma^2 \gamma_j^{(1)}\right], & j = l \end{cases} \tag{39}$$

where $\phi_j^{(k,l)}$ is as in (37).

Based on Lemmas 2–4, the linear MMSE detection can be performed from (32) and (33), and its performance can be evaluated. Although the expression in (39) is approximate, it is quite accurate for practical CM-TR UWB system parameters [33].

As will be investigated in Section 4.5, the linear MMSE receiver provides significant performance improvements over the conventional receiver and the chip discriminator. In addition, it can be implemented in practice based on the estimates of the correlation matrix of the energy samples. The main disadvantage of the linear MMSE receiver compared with the conventional receiver and the chip discriminator is its computational complexity because of the need for the matrix inversion operation to calculate the MMSE weight (see (31)). Because the dimension of the matrix is $N_\mathrm{f} \times N_\mathrm{f}$, the computational complexity can be high for a large number of frames. In those scenarios, the two-stage MMSE approach can be employed as in [34] in order to provide trade-offs between performance and computational complexity.

4.4. Maximum likelihood receiver

In this section, we obtain the ML receiver, which minimizes the probability of error and serves as a reference for the other receivers discussed in the previous sections.

The ML receiver estimates the information bits of all the users by maximizing the log-likelihood of the

observations in (16). That is, the set of information bits $\mathbf{b} = [b^{(1)} \cdots b^{(K)}]^T$ are estimated as

$$\hat{\mathbf{b}} = \arg\max_{\mathbf{b}} \log\left(p_{\mathbf{b}}(\mathbf{y})\right) = \arg\max_{\mathbf{b}} \sum_{j=0}^{N_f-1} \log\left(p_{\mathbf{b}}(y_j)\right), \tag{40}$$

where $p_{\mathbf{b}}(\mathbf{y})$ and $p_{\mathbf{b}}(y_j)$ denote, respectively, the conditional probability density functions (p.d.f.s) of $\mathbf{y}$ and y_j given $\mathbf{b}$. As for the single-user case, the noise components are assumed to be independent for energy samples from different frames, which is an accurate approximation in practice.

For a given set of signal parameters, the energy sample y_j is (noncentral) chi-square distributed; that is, $p_{\mathbf{b}}(y_j)$ is expressed as

$$p_{\mathbf{b}}(y_j) = \frac{1}{2\sigma^2}\left(\frac{y_j}{\theta_j(\mathbf{b})}\right)^{\frac{M}{4}-\frac{1}{2}} e^{-\frac{(\theta_j(\mathbf{b})+y_j)}{2\sigma^2}} \times I_{\frac{M}{2}-1}\left(\frac{\sqrt{\theta_j(\mathbf{b})\, y_j}}{\sigma^2}\right), \tag{41}$$

where $\theta_j(\mathbf{b})$ represents the signal energy in the absence of noise. Note that when $\theta_j(\mathbf{b}) = 0$, y_j reduces to a central chi-square random variable, and $p_{\mathbf{b}}(y_j)$ is given by $p_{\mathbf{b}}(y_j) = y_j^{\frac{M}{2}-1} e^{-\frac{y_j}{2\sigma^2}} / (\sigma^M 2^{\frac{M}{2}} \Gamma(M/2))$. Based on (41), the ML detector in (40) can be expressed as

$$\hat{\mathbf{b}} = \arg\max_{\mathbf{b}} \sum_{j=0}^{N_f-1} \left(\frac{M}{4}-\frac{1}{2}\right)\left[\log y_j - \log\left(\theta_j(\mathbf{b})\right)\right] - \frac{(\theta_j(\mathbf{b})+y_j)}{2\sigma^2} + \log\left\{I_{\frac{M}{2}-1}\left(\frac{\sqrt{\theta_j(\mathbf{b}) y_j}}{\sigma^2}\right)\right\}. \tag{42}$$

Note that the optimization should be performed over 2^K possible values of $\mathbf{b}$, which can result in very high complexity for a large number of users.

The expression in (42) provides an accurate expression for the ML detector. However, the objective function can be computationally complex to evaluate. Therefore, the Gaussian approximation [7,33] can be used to provide a simpler alternative solution. For large values of M, y_j can be approximated by a Gaussian distribution with mean μ_j and variance σ_j^2, which are given respectively by $\mu_j = \sigma^2 M + \theta_j(\mathbf{b})$ and $\sigma_j = 2M\sigma^4 + 4\sigma^2\theta_j(\mathbf{b})$. Then, the ML receiver in (40) can be expressed as

$$\hat{\mathbf{b}} = \arg\min_{\mathbf{b}} \sum_{j=0}^{N_f-1} \left\{\log(\sqrt{2\pi}\,\sigma_j) + \frac{(y_j-\mu_j)^2}{2\sigma_j^2}\right\}. \tag{43}$$

Although (43) is significantly simpler than (42), the implementation of the ML receiver may not be possible in practical CM-TR UWB systems because the channel state information, the TH sequences, the polarity, and orthogonalization codes for all users must be known by the user of interest in order to implement the ML receiver (namely, to be able to calculate $\theta_j(\mathbf{b})$). Therefore, the ML receiver can be considered to provide a performance benchmark for the other receivers.

4.5. Simulation results

In this section, simulation results are presented in order to compare the performance of the receivers considered in the previous sections. The UWB pulse $\omega(t)$ is chosen as the second order derivative of the Gaussian pulse [35]; that is, $\omega(t) = \left(1 - 4\pi t^2/\zeta^2\right) e^{-\frac{2\pi t^2}{\zeta^2}} / \sqrt{E_p}$, where E_p is a scalar chosen to set $\omega(t)$ to unit energy, and $\zeta = T_c/2.5$ determines the pulse width [16]. The bandwidth of the receive filter is set to 5 GHz, and the channel statistics are obtained from the IEEE 802.15.4a channel models CM1 (residential line-of-sight), CM2 (residential nonline-of-sight), CM3 (office line-of-sight), and CM4 (office nonline-of-sight). Please refer to [29] and [36] for the details of the channel models. For the considered CM-TR UWB system, the system parameters are chosen as $N_f = 4$ and $N_c = 250$, which correspond to a data rate of $R_b = 1$ Mbps. Also, the chip duration T_c is set to 1 ns. In order to prevent catastrophic collisions between pulses of different users, TH sequences are employed for each user. To avoid IFI, the TH sequences are chosen uniformly from the set $\{0, 1, \ldots, x\}$, where x is set to 130, 110, 160, and 170 for CM1, CM2, CM3, and CM4, respectively. In addition, the orthogonalization codes are selected independently and randomly for different users.

In the simulations, a two-user scenario is studied, where $E_1 = 1$ and $E_2 = 2$, and user 1 is considered as the user of interest. In order to provide a fair performance comparison of different receivers, the optimal integration interval is employed in each receiver. Considering the same integration duration for all the frames of a given receiver, the duration of the integration interval, $|\Gamma|$, is optimized for a practical SNR value, which is selected as 12 dB

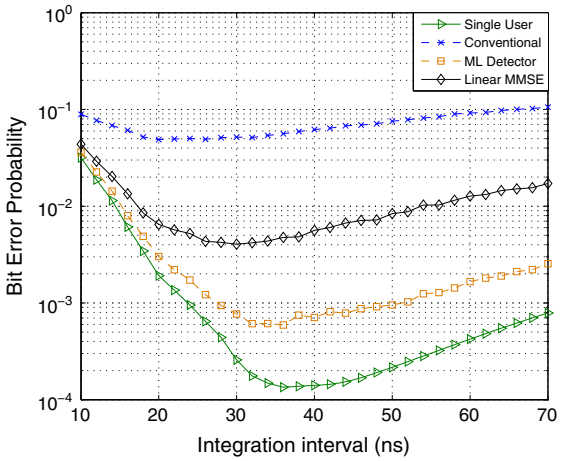

Figure 3. Bit error probability versus $|\Gamma|$ for CM4 with $N_f = 4$ and $N_c = 250$ at a signal-to-noise ratio of 12 dB.

in the simulations. As an example illustration, Figure 3 indicates that there exists an optimal integration interval that minimizes the BEP for each receiver. Such a behavior is expected because small integration intervals cannot collect sufficient signal energy from the multipath components, and large integration intervals increase the effects of noise/interference in the energy samples.

Figures 4–7 illustrate the BEP versus SNR curves for CM1, CM2, CM3, and CM4, respectively, for various receivers. Also, the single-user performance is shown for comparison purposes. In the figures, the SNR is defined in terms of E_h/N_0, where E_h is defined as $\int_\Gamma h^2(t)\,dt$, with $h(t) = \sqrt{E_1/(2N_f)}\,\tilde{\omega}(t)$ and $\tilde{\omega}(t)$ denoting the response of the channel to the UWB pulse $\omega(t)$. This SNR definition is adopted in order to be in compliance with [5] and [7]. For the chip discriminator, threshold Δ_1 in (20) is set to 14, 20, 10, and 19, respectively; for CM1, CM2, CM3, and CM4, Δ_2 is set to 1 for all the cases. These

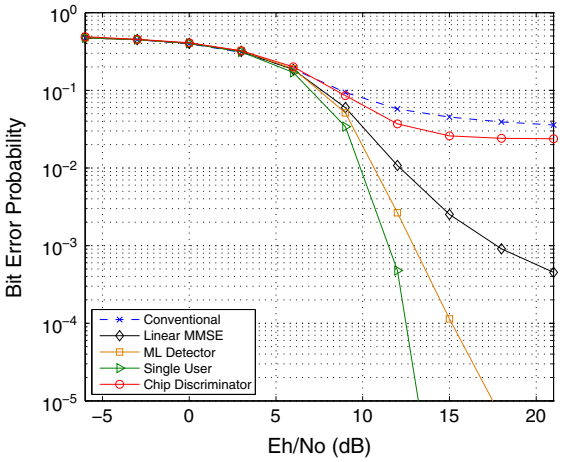

Figure 4. Bit error probability versus E_h/N_0 for a two-user system for CM1 with $N_f = 4$, $N_c = 250$, $E_1 = 1$, and $E_2 = 2$.

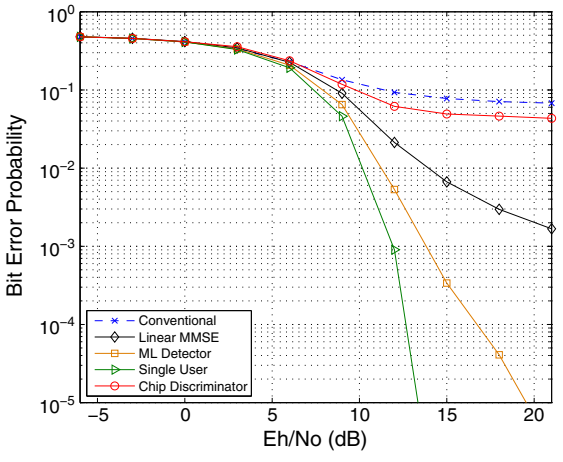

Figure 5. Bit error probability versus E_h/N_0 for a two-user system for CM2 with $N_f = 4$, $N_c = 250$, $E_1 = 1$, and $E_2 = 2$.

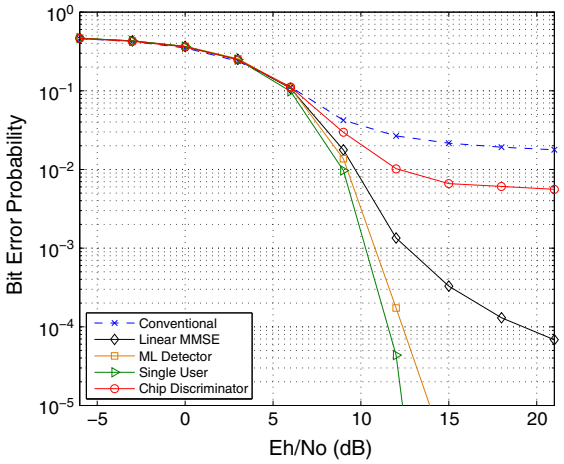

Figure 6. Bit error probability versus E_h/N_0 for a two-user system for CM3 with $N_f = 4$, $N_c = 250$, $E_1 = 1$, and $E_2 = 2$.

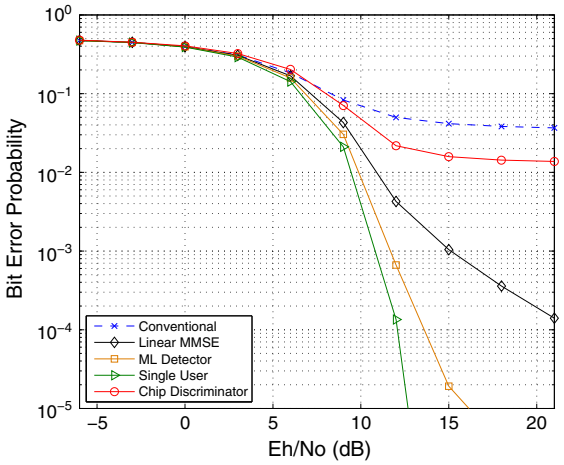

Figure 7. Bit error probability versus E_h/N_0 for a two-user system for CM4 with $N_f = 4$, $N_c = 250$, $E_1 = 1$, and $E_2 = 2$.

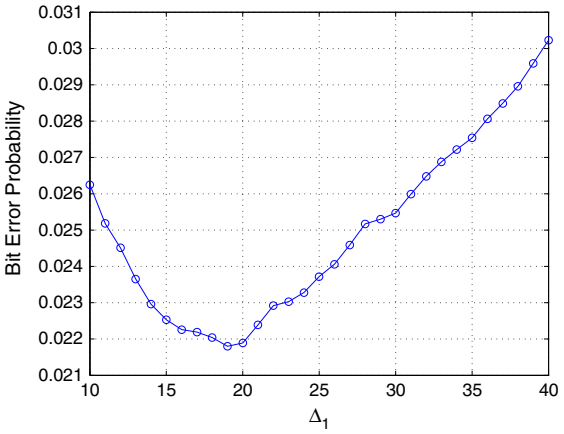

Figure 8. Bit error probability versus Δ_1 for the chip discriminator in CM4 with $N_f = 4$ and $N_c = 250$.

Table I. Bit error probabilities for CM1, CM2, CM3, and CM4 channel models in a two-user system ($E_1 = 1$ and $E_2 = 2$) at a signal-to-noise ratio of 12 dB.

Channel model	Average RMS delay spread (ns)	Single user ($\times 10^{-3}$)	ML detector ($\times 10^{-3}$)	MMSE receiver ($\times 10^{-3}$)	Chip Discr. ($\times 10^{-3}$)	Conven. receiver ($\times 10^{-3}$)
CM1	16.8	0.48	2.65	10.8	36.9	57.5
CM2	19.3	0.90	5.32	21.2	61.7	92.8
CM3	9.96	0.04	0.17	1.34	10.2	26.6
CM4	12.8	0.13	0.66	4.26	21.8	49.9

RMS, root-mean-square; ML, maximum likelihood ; MMSE, minimum mean-squared error.

values are selected among other options in order to optimize the performance of the chip discriminator. As an example illustration, Figure 8 plots the BEP versus Δ_1, which shows that $\Delta_1 = 19$ optimizes the performance for CM4. From Figures 4–7, it is observed that the ML receiver has the best performance as expected. The linear MMSE receiver performs worse than the ML receiver, but it provides significant performance improvements over the conventional receiver and the chip discriminator. Also, it is observed that the chip discriminator performs better than the conventional receiver for all the channels. This is mainly because of the fact that the chip discriminator can obtain uncorrupted or slightly corrupted pulses in this case because there is only one interfering user.[‖] Furthermore, it is observed that the residential environments (CM1 and CM2) present more challenging channel conditions than the office environments (CM3 and CM4), and result in larger bit error probabilities. In addition, as expected, the BEPs are lower in line-of-sight scenarios than those in nonline-of-sight scenarios, which can be observed by comparing Figure 4 with Figure 5, or Figure 6 with Figure 7.

In order to compare the performance of the receivers against the delay spreads of different channels, Table I presents the BEPs at an SNR of 12 dB. It is observed from the table that the performance of all the receivers degrades as the average root-mean-square (RMS) delay spread of the channel increases. (RMS delays spreads are averaged over 100 channel realizations for each channel model.) Specifically, CM3 has an average RMS delay spread of about 10 ns, and achieves the lowest BEPs, whereas CM2 has the highest BEPs with an average RMS delay spread of around 19 ns.

Finally, the BEPs of the conventional receiver, the chip discriminator, and the linear MMSE receiver are plotted versus the number of users in Figure 9 for CM3 in the absence of background noise. The user of interest has $E_1 = 1$, whereas the interfering users have $E_k = 2$ for $k = 2, \ldots, K$. In other words, a scenario with significant multiple access interference is considered. It is observed that the linear MMSE receiver achieves the lowest BEPs in all cases, and the chip discriminator outperforms the conventional receiver.

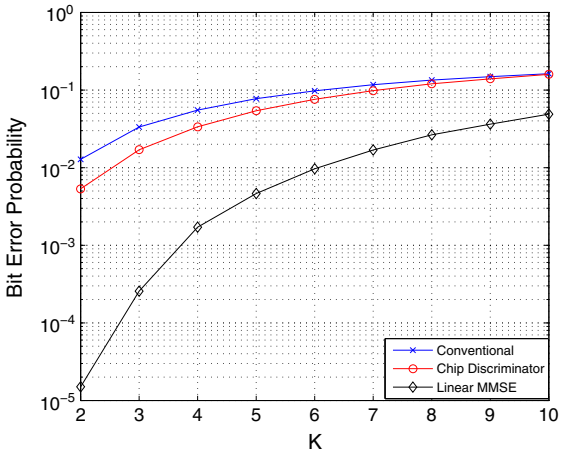

Figure 9. Bit error probability versus the number of users (K) for CM3 in the absence of background noise with $N_f = 4$, $N_c = 250$, $E_1 = 1$, and $E_k = 2$ for $k = 2, \ldots, K$.

5. CONCLUDING REMARKS

In this study, optimal and suboptimal receivers have been investigated for single-user and multi-user CM-TR UWB systems. For single-user systems, it has been shown that the conventional receiver performs very closely to the optimal receiver; hence, it is a natural choice for CM-TR systems because of its low complexity. On the other hand, it has been observed that the conventional receiver can perform very poorly in multi-user environments, and improved performance can be achieved by using the chip discriminator, which discards some energy samples with significant interference. However, the performance can still be unacceptable in certain cases (e.g., Figure 4 and Figure 5). Therefore, the linear MMSE receiver has been proposed, and it has been shown to perform significantly better

[‖]Simulations are performed also for a three-user system with $E_1 = E_2 = E_3 = 1$, and the conventional receiver and the chip discriminator are observed to perform very closely for all the channel models in that case (figures not shown here). This is because of the fact that there occur frequent pulse collisions in the three-user system considering the channel models and the frame duration; hence, the chip discriminator may not obtain uncorrupted or slightly corrupted pulses in many cases and operates similarly to the conventional receiver.

than the conventional receiver and the chip discriminator. In addition, the practicality of its implementation has been discussed. Finally, the ML receiver has been obtained, which achieves the lowest BEPs but is impractical for CM-TR UWB systems in most cases. Therefore, the linear MMSE receiver has been shown to be a good choice for multi-user CM-TR UWB systems. Although not investigated in this study, selection of the orthogonalization codes can be optimized similarly to [12] in order to improve the performance of the proposed receivers, which is considered as a possible topic for future work.

APPENDICES

A. Proof of Proposition 1. For equiprobable information symbols, the ML decision rule minimizes the average probability of error, which can be expressed as [21]

$$p_1(\mathbf{y}) \underset{\hat{b}=-1}{\overset{\hat{b}=+1}{\gtrless}} p_0(\mathbf{y}) , \tag{44}$$

where $\mathbf{y} = [y_0\ y_1 \cdots y_{N_f-1}]$, and $p_i(\mathbf{y})$ is the conditional probability density function of $\mathbf{y}$ given that the hypothesis $\mathcal{H}_i$ is true ($i = 0, 1$).

From the independent noise components assumption, $p_1(\mathbf{y})$ can be obtained, using (12), as

$$p_1(\mathbf{y}) = \prod_{j\in\mathcal{S}} \frac{1}{2\sigma^2} \left(\frac{y_j}{\theta}\right)^{\frac{M}{4}-\frac{1}{2}} e^{-\frac{(\theta+y_j)}{2\sigma^2}} \times \mathrm{I}_{\frac{M}{2}-1}\left(\frac{\sqrt{\theta y_j}}{\sigma^2}\right) \prod_{j\in\bar{\mathcal{S}}} \frac{y_j^{\frac{M}{2}-1} e^{-\frac{y_j}{2\sigma^2}}}{\sigma^M 2^{\frac{M}{2}} \Gamma(M/2)} , \tag{45}$$

where $\Gamma(\cdot)$ is the Gamma function [20] and

$$\mathrm{I}_\nu(x) = \sum_{l=0}^{\infty} \frac{(x/2)^{\nu+2l}}{l!\,\Gamma(\nu+l+1)} \tag{46}$$

for $x \geq 0$ is the ν-th order modified Bessel function of the first kind.

For $p_0(\mathbf{y})$, the expression in (45) can be used by replacing $\mathcal{S}$ and $\bar{\mathcal{S}}$. Then, (44) can be shown to be equal to (13) after some manipulation. □

B. Proof of Lemma 1. From (46), the decision rule in (13) can be expressed as

$$\prod_{j\in\mathcal{S}} y_j^{\frac{1}{2}-\frac{M}{4}} f_\theta(y_j) \underset{\hat{b}=-1}{\overset{\hat{b}=+1}{\gtrless}} \prod_{j\in\bar{\mathcal{S}}} y_j^{\frac{1}{2}-\frac{M}{4}} f_\theta(y_j) \tag{47}$$

where

$$f_\theta(y_j) = \sum_{l=0}^{\infty} \frac{(\theta y_j)^{\frac{M}{4}-\frac{1}{2}+l}}{(2\sigma^2)^{\frac{M}{2}-1+2l} l!\,\Gamma(M/2+l)} . \tag{48}$$

From the facts that $|\mathcal{S}| = |\bar{\mathcal{S}}| = N_f/2$ and $\Gamma(M/2+l) = (M/2+l-1)!$ (because $M/2$ is an integer), (47) and (48) can be simplified, after some manipulation, to

$$\prod_{j\in\mathcal{S}} \sum_{l=0}^{\infty} k_l \theta^l y_j^l \underset{\hat{b}=-1}{\overset{\hat{b}=+1}{\gtrless}} \prod_{j\in\bar{\mathcal{S}}} \sum_{l=0}^{\infty} k_l \theta^l y_j^l , \tag{49}$$

where k_l is given by (15) for $l = 0, 1, 2, \ldots$. Then, (14) can be obtained by taking the logarithm of both sides in (49) and using the fact that $k_0 = 1$. □

REFERENCES

1. Arslan H, Chen ZN, Di Benedetto M-G (eds). *Ultra Wideband Wireless Communications Systems*. Wiley-Interscience: Hoboken, 2006.
2. Sahinoglu Z, Gezici S, Guvenc I. *Ultra-Wideband Positioning Systems: Theoretical Limits, Ranging Algorithms, and Protocols*. Cambridge University Press: New York, 2008.
3. Hoctor R, Tomlinson H. Delay-hopped transmitted-reference RF communications. In *Proceedings of the IEEE Conference on Ultra Wideband Systems and Technologies*, Baltimore, MD, USA, May 2002; 265–269.
4. Choi JD, Stark WE. Performance of ultra-wideband communications with suboptimal receivers in multipath channels. *IEEE Journal on Selected Areas in Communications* Dec. 2002; **20**: 1754–1766.
5. Goeckel DL, Zhang Q. Slightly frequency-shifted reference ultra-wideband (UWB) radio. *IEEE Transactions on Communications* Mar. 2007; **55**: 508–519.
6. Zhang J, Hu H, Liu L, Li T. Code-orthogonalized transmitted-reference ultra-wideband (UWB) wireless communication system. In *Proceedings of the International Conference on Wireless Communications, Networking and Mobile Computing*, Shanghai, Sept. 2007; 528–532.
7. D'Amico AA, Mengali U. Code-multiplexed UWB transmitted-reference radio. *IEEE Transactions on Communications* Dec. 2008; **56**: 2125–2132.
8. Zhang J, Hu H-Y, Zhang Z-Y. Timing acquisition for code-orthogonalized transmitted-reference ultra-wideband (UWB) wireless communication system. In *Proceedings of the IEEE International Workshop on Radio-Frequency Integration Technology*, Singapore, Dec. 2007; 50–53.
9. Goeckel DL, Mehlman J, Burkhart J. A class of ultra wideband (UWB) systems with simple receivers. In *Proceedings of the IEEE Military Communications Conference (MILCOM)*, Orlando, FL, USA, Oct. 2007; 1–7.

10. Nie H, Chen Z. Differential code-shifted reference ultra-wideband (UWB) radio. In *Proceedings of the 68th IEEE Vehicular Technology Conference*, Calgary, Sept. 2008; 1–5.
11. Nie H, Chen Z. Code-shifted reference ultra-wideband (UWB) radio. In *Proceedings of the 6th Annual Conference on Communication Networks and Services Research*, Halifax, Nova Scotia, Canada, May 2008; 385–389.
12. D'Amico AA, Mengali U. Code-multiplexed transmitted-reference UWB systems in a multi-user environment. *IEEE Transactions on Communications* Mar. 2010; **58**: 966–974.
13. Kim DI, Jia T. M-ary orthogonal coded/balanced ultra-wideband transmitted-reference systems in multipath. *IEEE Transactions on Communications* Jan. 2008; **56**: 102–111.
14. Jia T, Kim DI. Multiple access performance of balanced UWB transmitted-reference systems in multipath. *IEEE Transactions on Wireless Communications* Mar. 2008; **7**: 1084–1094.
15. Guvenc I, Arslan H. A review on multiple access interference cancellation and avoidance for ir-uwb. *Signal Processing* 2007; **87**(4): 623–653.
16. Gezici S, Kobayashi H, Poor HV, Molisch AF. Performance evaluation of impulse radio UWB systems with pulse-based polarity randomization. *IEEE Transactions on Signal Processing* July 2005; **53**: 2537–2549.
17. Nakache Y-P, Molisch AF. Spectral shape of UWB signals – influence of modulation format, multiple access scheme and pulse shape. In *Proceedings of the 57th IEEE Vehicular Technology Conference*, Vol. 4, Jeju, Korea, Apr. 2003; 2510–2514.
18. Win MZ, Scholtz RA. Impulse radio: how it works. *IEEE Communications Letters* 1998; **2**(2): 36–38.
19. D'Amico AA, Mengali U. Multiuser UWB communication systems with code-multiplexed transmitted reference. In *Proceedings of the IEEE International Conference on Communications (ICC)*, Beijing, China, May 2008; 3765–3769.
20. Proakis JG, Digital Communications, 4th ed. McGraw-Hill: New York, 2001.
21. Poor HV. *An Introduction to Signal Detection and Estimation*. Springer-Verlag: New York, 1994.
22. Humblet PA, Azizoglu M. On the bit error rate of lightwave systems with optical amplifiers. *Journal of Lightwave Technology* Nov. 1991; **9**: 1576–1582.
23. Tian Z, Sadler BM. Weighted energy detection of ultra-wideband signals. In *Proceedings of the 6th IEEE Workshop on Signal Processing Advances in Wireless Communications*, New York, USA, June 2005; 1068–1072.
24. Tutay ME, Gezici S. Performance analysis of code-multiplexed transmitted-reference ultra-wideband systems. In *Proceedings of the IEEE International Conference on Ultra-Wideband (ICUWB)*, Bologna, Italy, Sept. 2011.
25. Fishler E, Poor HV. Low-complexity multiuser detectors for time-hopping impulse-radio systems. *IEEE Transactions on Signal Processing* Sept. 2004; **52**: 2561–2571.
26. Gezici S, Kobayashi H, Poor HV. A comparative study of pulse combining schemes for impulse radio UWB systems. In *Proceedings of the IEEE Sarnoff Symposium on Advances in Wired and Wireless Communication*, Princeton, NJ, Apr. 2004; 7–10.
27. Goldsmith A, Wireless Communications. Cambridge University Press: Cambridge, UK, 2005.
28. Cassioli D, Win MZ, Molisch AF. The ultra-wide bandwidth indoor channel: from statistical model to simulations. *IEEE Journal on Selected Areas in Communications* Aug. 2002; **20**: 1247–1257.
29. Molisch AF, Balakrishnan K, Chong C-C, Emami S, Fort A, Karedal J, Kunisch J, Schantz H, Schuster U, Siwiak K. 802.15.4a channel model - final report. *tech. rep., IEEE*, 2005.
30. Win MZ, Scholtz RA. On the energy capture of ultra-wide bandwidth signals in dense multipath environments. *IEEE Communications Letters* Sept. 1998; **2**: 245–247.
31. Cassioli D, Win MZ, Vatalaro F, Molisch AF. Low complexity rake receivers in ultra-wideband channels. *IEEE Transactions on Wireless Communications* Apr. 2007; **6**: 1265–1275.
32. Verdu S. *Multiuser Detection*, 1st ed. Cambridge University Press: Cambridge, UK, 1998.
33. Tutay ME. Receiver design and performance analysis for code-multiplexed transmitted-reference ultra-wideband systems, *M.S. Thesis*, Bilkent University, Aug. 2010. http://www.ee.bilkent.edu.tr/∼gezici/thesisMET.pdf.
34. Gezici S, Molisch AF, Kobayashi H, Poor HV. Low-complexity MMSE combining for linear impulse radio UWB receivers. In *Proceedings of the IEEE International Conference on Communications*, Istanbul, Turkey, June 2006.
35. Ramirez-Mireles F, Scholtz RA. Multiple-access performance limits with time hopping and pulse position modulation. In *Proceedings of the IEEE Military Communications Conference*, Vol. 2, Bedford, MA, USA, Oct. 1998; 529–533.
36. Molisch AF, *et al*. A comprehensive standardized model for ultrawideband propagation channels. *IEEE Transactions on Antennas and Propagation* Nov. 2006; **54**: 3151–3166.

AUTHORS' BIOGRAPHIES

Sinan Gezici received the B.S. degree from Bilkent University, Turkey in 2001, and the Ph.D. degree in Electrical Engineering from Princeton University in 2006. From 2006 to 2007, he worked at Mitsubishi Electric Research Laboratories, Cambridge, MA. Since February 2007, he has been an Assistant Professor in the Department of Electrical and Electronics Engineering at Bilkent University. Dr. Gezici's research interests are in the areas of signal detection, estimation and optimization theory, and their applications to wireless communications and localization systems. Among his publications in these areas is the book Ultra-wideband Positioning Systems: Theoretical Limits, Ranging Algorithms, and Protocols (Cambridge University Press, 2008).

Mehmet Emin Tutay received the B.S. degree in 2008 and the M.S. degree in 2010, both from Bilkent University, Turkey. He is currently working towards the Ph.D. degree in the Department of Electrical and Electronics Engineering, Bilkent University. His main research interests are in the fields of statistical signal processing and wireless communications.